John von Neumann Institute for Computing

Phase Transitions in Macromolecular Systems: Monte Carlo and Molecular Dynamics Simulations of Coarse Grained Models

Kurt Binder, Jörg Baschnagel, Marcus Müller,
Wolfgang Paul

published in

NIC Symposium 2001, Proceedings,
Horst Rollnik, Dietrich Wolf (Editor),
John von Neumann Institute for Computing, Jülich,
NIC Series, Vol. **9**, ISBN 3-00-009055-X, pp. 363-372, 2002.

http://www.fz-juelich.de/nic-series/volume9

Phase Transitions in Macromolecular Systems: Monte Carlo and Molecular Dynamics Simulations of Coarse Grained Models

Kurt Binder[1], **Jörg Baschnagel**[2], **Marcus Müller**[1], **and Wolfgang Paul**[1]

[1] Institut für Physik, Johannes Gutenberg Universität Mainz
Staudinger Weg 7, 55099 Mainz, Germany

[2] Institut Charles Sadron, Université Louis Pasteur
6 rue Boussingault, 67087 Strasbourg, France

The study of phase transitions that occur in dense polymer systems (glass transition; unmixing and wetting transitions in polymer mixtures; mesophase ordering in block copolymer melts) is very difficult, because due to the flexibility of large macromolecules there is a complicated interplay between entropic and enthalpic effects. Due to the many length scales involved in these problems, and the slow relaxation of long chain molecules, computer simulations cannot study these phenomena in full atomistic detail, but need to use coarse-grained models. Two such models, the bond fluctuations model on the lattice, and the bead-spring model in the continuum, will be described, and it will be shown that simulations of these models can help to better understand the phase behavior of polymeric materials. As characteristic examples, we shall mention static and dynamic properties of the glass transition, capillary waves of interfaces and between coexisting unmixed phases in polymer blends, and block copolymers confined between walls and their transition from parallel to perpendicular orientation of the lamellae.

1 Introduction

Macromolecules are not only the constituents of all living bodies, but are also the ingredients of the plastic materials which now are ubiquitously used. The theoretical understanding of such polymeric systems hence is of utmost importance, but also is very difficult since even the simplest polymers, linear homopolymers being formed by a succession of identical repeat units (="monomers"), exhibit structure from the scale of a chemical covalent bond (≈ 1 Å) up to the size of the random-walk like coil (≈ 100 Å, cf. Fig. 1). These polymer coils (in solution or melt) are very soft objects: Note that the end-to-end distance

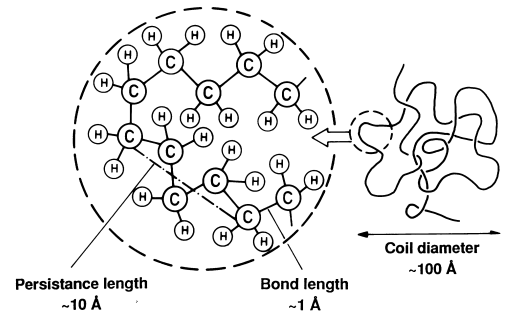

Figure 1. Length scales describing the structure of a long polymer coil. Note that the "persistence length" describes the scale on which correlations between bond orientations along the backbone of the polymer decay. The example shown here refers to polyethylene, $C_{N_P}H_{2N_P+2}$, where $N_P - 2$ repeat units CH_2 are linked together (with CH_3 groups at the chain ends).

R of a random walk of N steps of step length b is $R = bN^{1/2}$, so the volume taken by a coil is $V = 4\pi R^3/3 = 4\pi b^3/3N^{3/2}$, but the density of the effective monomeric units represented by the individual steps of the walk inside this volume is quite small, $\rho = N/V \propto b^{-3}N^{-1/2} \to 0$ for $N \to \infty$[1]. Therefore in a dense melt each polymer coil is interpenetrated by many other coils taking to some extent the same volume, and interactions between the monomers of a coil with other polymers or with external fields (e.g. due to walls or interfaces) may lead to a significant deformation of the configuration of such a chain molecule. Therefore the interplay between configurational entropy and enthalpy is a subtle matter for polymeric systems and analytical theories can provide only a limited understanding. Although thus the use of computer simulation to understand such systems is very desirable, the complicated geometrical structure (Fig. 1) and the associated very slow relaxation of the configuration of such macromolecules are severe obstacles for a viable simulation, too! However, some aspects of this difficulty can be overcome by introducing very simplified, coarse grained models which disregard chemical detail but focus on "universal" properties of polymer chains, such as chain connectivity plus "excluded volume" interactions (no two monomers can sit precisely on top of each other). The idea behind such models is to integrate several (e.g. $n = 5$) successive monomers along the backbone of a chain into one "effective bond" connecting "effective monomers". Thus the length b mentioned above is not the length of a covalent chemical bond, but rather a "mesoscopic length" (e.g. of the order of the "persistence length"), and the number N of such effective bonds is not the degree of polymerization $N_{\rm p}$ but only $N = N_{\rm p}/n$. Also the interaction potentials are very much simplified – while the force field for a chemically realistic description of a polymer is very complicated, potentials depending on bond lengths, bond angles, torsional angles etc., for the coarse grained model one may choose a simple anharmonic spring potential along the chain and a Lennard-Jones potential among non-bonded monomers (Fig. 2)[2]. This model is not only very well suited to investigate the glass transition of polymer melts by Molecular Dynamics simulations[2–8] (Sec. 2), but it can also be used to model phase separation between polymer rich and polymer poor phases in bad solvents[9], and to study the structure of wetting layers adsorbed on surfaces[9,10] etc.

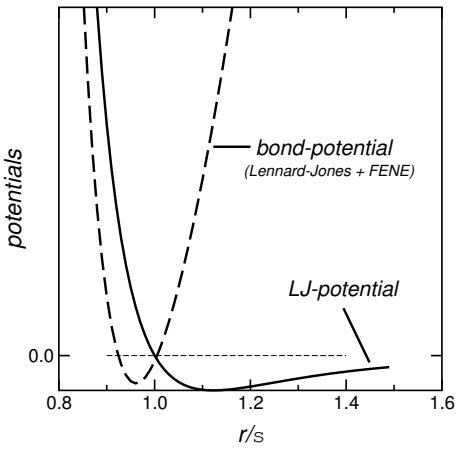

Figure 2. Effective bond potential (broken curve) and Lennard Jones (LJ) potential (full curve) plotted versus distance between effective monomers (left part). The LJ potential depends on the distance r between effective monomers as $U_{\rm LJ}(r) = 4\epsilon[(\sigma/r)^{12} - (\sigma/r)^6]$, and one chooses its strength ϵ as the unit of energy scale ($\epsilon \equiv 1$) and its range σ as unit of length scale ($\sigma \equiv 1$). The bond potential (see Ref.[2] for its precise definition) is chosen such that its minimum position ($\ell_{\rm min} \approx 0.96$) is smaller than that of the LJ potential (≈ 1.13). This incompatibility prevents the formation of a regular crystalline structure at low temperatures, even for short chains (mostly we use $N = 10$).

An alternative model, well suited for Monte Carlo simulations is the bond fluctuation model on the simple cubic lattice[11–20]. In this model, an effective monomer blocks all eight sites of an elementary cube on the lattice, and effective bonds between subsequent monomers are allowed to take the lengths $b = 2$, $\sqrt{5}$, $\sqrt{6}$, 3 and $\sqrt{10}$ (for this model the lattice spacing is taken as the unit of length). If one wishes to model the glass transition of polymers, one chooses an energy function $\mathcal{H}(b)$ depending on the length b[8,12–14]: the choice $\mathcal{H}(b = 3) = 0$ while $\mathcal{H}(b \neq 3) = \epsilon = 1$ has the effect that bonds taking their minimum energy length ($b = 3$, which should happen at low temperature, since the system should approach its ground state then) waste "free volume", 4 lattice sites per bond being then not accessible for occupation by any monomers. In a dense system, not enough free volume is available that all bonds can reach their ground state easily, some bonds remain blocked in unfavorable states, and this "geometric frustration" is enough to cause a glass transition.

Alternatively, when one wishes to model a binary mixture of two types of polymers (which we denote as A and B here), we may take energy parameters $\epsilon_{\mathrm{AA}},\ \epsilon_{\mathrm{AB}}$ and ϵ_{BB} between different pairs of monomers, to simulate non-bonded interactions, and the unmixing behavior that results[15–20] (Sec. 3a). In this case, we arbitrarily choose $\mathcal{H}(b) \equiv 0$, to avoid complications due to glass-like behavior at low temperatures (unlike real polymers, where the complication of the glass transition or crystallization can never be avoided!). It is a big advantage of simulations, however, that one can focus on one physical phenomenon at a time, "switching off" interaction energies that would complicate matters, and reach a step-by-step understanding of the very complicated materials. In the conclusions (Sec. 5) we shall give some further comments on this strategy.

2 Simulation of the Glass Transition of Polymers

As has been emphasized in the introduction, many complicated features of real polymers have been disregarded from the start by the choice of a very simplified model. Therefore it is important to first validate the model, showing that it still reproduces all the important phenomena known from experiment. Thus, Fig. 3a shows that the specific volume of the supercooled polymer melt shows a kink at a temperature $T_{\mathrm{g}} \approx 0.41$ (remember that $\epsilon \equiv 1$ for the model of Fig. 2, and we also choose Boltzmann's constant $k_{\mathrm{B}} \equiv 1$, so our temperature variable T is dimensionless), while in that regime the structure factor $S(q)$ of the melt changes only very little. As discussed in more detail in the recent review[8], the simulation "data" shown in Fig. 3b exhibit a striking similarity to corresponding experiments. Therefore, it makes sense to examine the model more closely and study the slowing down of various properties as the glass transition is approached.

Due to this slowing down, very long Molecular Dynamics runs (extending up to 8 decades in time) are required, and since the configurations generated are highly correlated with each other, many equivalent "replicas" of the same system must be run in parallel and their properties must be averaged over, in order to obtain sufficiently accurate and statistically significant information. It is this high computational effort which necessitates the use of large scale supercomputer facilities such as the CRAY-T3E of the NIC Jülich.

Fig. 4 shows a typical example of the type of simulation results that can be obtained: Since many quantities (various mean square displacements, coherent and incoherent scattering functions, etc.) can be obtained for the same model simultaneously and with very

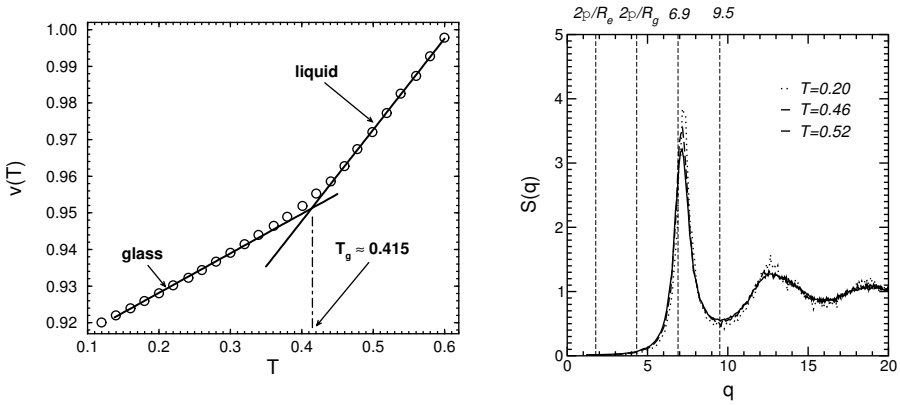

Figure 3. a) Volume $v(T)$ per effective monomer in a slow cooling computer experiment, starting at a pressure $p = 1$ (all variables are in Lennard-Jones units defined by $\epsilon = 1, \sigma = 1$) from a well-equilibrated configuration at $T = 0.6$, and lowering T every 500 000 MD time steps by 0.02, using the model of Fig. 2. b) Plot of the collective static structure factor $S(q)$ vs wave number for three temperatures $T = 0.2$ (deep in the glass phase), $T = 0.46$ (in the fluid a little bit above the glass transition temperature $T_{\rm g}$, and $T = 0.52$, where the model behaves as a "normal" fluid polymer melt. Dashed lines indicate inverse characteristic length scales: $R_{\rm e}$ is the end-to-end distance of the chains, $R_{\rm g}$ their gyration radius, and also the position of the first peak (the so-called "amorphous halo", at $q = 6.9$) and the subsequent minimum (at $q = 9.5$) are highlighted. While the first peak of $S(q)$ yields information on the packing of the effective monomers in the melt, the second and third peak are due to intrachain correlations between monomers. Note that experimentally $S(q)$ is accessible via the scattering intensity of x-rays or neutrons observed under scattering angle θ related to q by $q = (4\pi/\lambda)\sin\theta$, λ being the wavelength of the radiation. From Baschnagel et al.[6].

good precision, a more stringent test of theories is possible with such simulations than with corresponding experiments. In particular, simulations such as shown in Fig. 4 could provide a compelling test[7] of the so-called "mode-coupling theory"[21] of the glass transition which describes the blocking of diffusive motions of an atom in a dense fluid by the cage formed by its neighbors.

Of course, the question to what extent results from a model calculation are universal or reflect particular properties of a model is always a matter of concern. Therefore it is gratifying that very similar results on the glass transition of polymer melts could in fact be deduced from a rather different model, namely the bond fluctuation model on the simple cubic lattice[13]. The diffusive motion of effective monomers there is modeled in the framework of a Monte Carlo simulation by choosing effective monomers at random and attempting to displace them by a lattice unit in randomly chosen directions. Moreover, for this model the notion of a configurational entropy of the melt has a well-defined meaning, thus allowing a stringent test[14] of the "entropy theory"[22,23] of the glass transition. According to this theory, the transition from the undercooled fluid to an underlying "ideal glass" (which is not realized experimentally, because the system falls out of thermodynamic equilibrium before it reaches this ideal phase transition) occurs when the configurational entropy of the fluid vanishes (thus the "entropy catastrophe" of a negative configurational entropy is avoided). Fig. 5 shows now the configurational entropy of the bond fluctuation model in comparison with the theoretical predictions of Gibbs and di Marzio[22], Flory[23] and Milchev[24]. One sees that these theories are rather unreliable, and while there is indeed

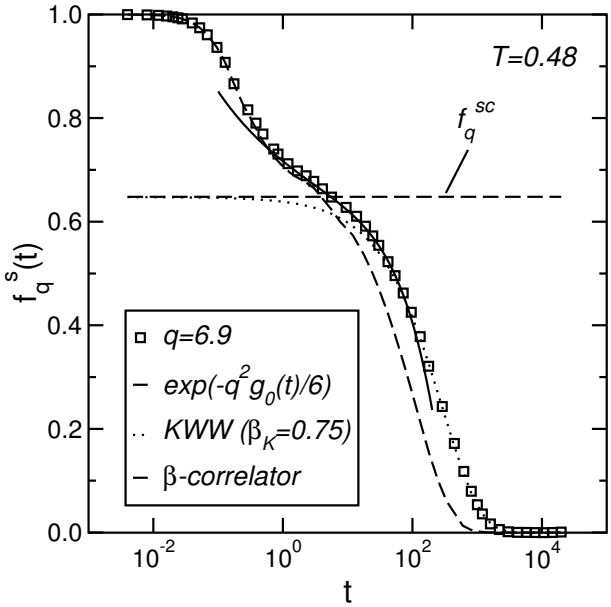

Figure 4. Incoherent intermediate scattering function $\phi_q^{\rm s}(t) = (1/\mathcal{N}) \sum \langle \exp\{{\rm i}\vec{q} \cdot [\vec{r}_j(t) - \vec{r}_j(0)]\} \rangle_T$ of the model of Fig. 2 plotted vs. time (in the Molecular Dynamics time units of $t_0 = (m\sigma^2/\epsilon)^{1/2}$, where the mass of effective monomeric units is set to unity as well). Here the sum over j is extended over all $\mathcal{N}$ monomeric units in the simulation box (typically $\mathcal{N} = 1200$, and periodic boundary conditions are used), $\vec{r}_j(t)$ being the position of the j-th monomer unit at time t. The wave number $q = 6.9$ is chosen, corresponding to the peak position in Fig. 3b, in order to study the dynamics of a particle associated with the "cage" of its nearest neighbors surrounding it. Several theoretical approximations are included: the approximation that all density fluctuations are Gaussian distributed amounts to $\phi_q^{\rm s}(t) = \exp[-q^2 g_0(t)/6]$, with $g_0(t)$ the mean square displacement of monomers after time t. This approximation describes only the early stages of relaxation, where a particle is still well confined in its "cage" (broken curve). The curve marked "β-correlator" describes the result of a mode coupling analysis, for the relaxation towards a plateau (described by the "nonergodicity parameter" $f_q^{\rm s}$) and its initial decay with the asymptotic decay is described by the "α-relaxation", namely a decay with the so-called KWW stretched exponential relaxation, $\phi_q^{\rm s}(t) \propto \exp[-(t/\tau)^{\beta_{\rm K}}]$, with $\beta_{\rm K} \approx 0.75$. Repeating this analysis at a range of temperature (the present figure refers to $T = 0.48$), one finds that the relaxation time τ scales as $\tau \propto (T/T_{\rm c} - 1)^{-\gamma}$, with $\gamma \approx 2.1$, $T_{\rm c} \approx 0.45$. This behavior is well compatible with predictions of the mode coupling theory (MCT). From Baschnagel et al.[6].

a strong decrease of the configurational entropy as the temperature is lowered, the simulations do not yield any evidence for an entropy catastrophe, suggesting that the latter is an artificial result due to bad approximations.

3 Interfaces between Coexisting Phases in Unmixed Polymer Blends

Polymer mixtures are technologically very important since mixing several polymers together often improves the physical properties of the resulting material. However, due to chain connectivity the configurational entropy is smaller by a factor of $1/N$, in comparison with a small molecule mixture. Therefore many polymer mixtures are not homogeneous on atomistic length scales, but rather phase separation in a binary (A,B) mixture has occurred,

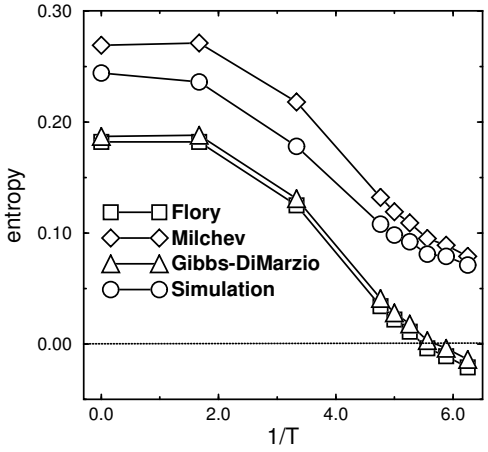

Figure 5. Entropy per lattice site for the bond fluctuation model of a polymer melt (chain length $N = 10$), plotted vs inverse temperature. Open circles are the simulation results of Wolfgardt et al.[14], while the other symbols show the predictions of the various theories[22–24]. Note that the input parameters of these theories can also be extracted from the same simulations[14], so the theories do not contain any adjustable parameters. Since the simulation[8,13] show that for this model $T_c \approx 0.15$, which is an upper bound for the actual glass transition temperature, the entropy vanishing at $T_0 \approx 0.18$ in this figure is an artefact provided by too inaccurate approximations of[22,23] for the entropy. Indeed, most of this error already occurs for infinite temperature ($1/T = 0$), the actual entropy being severely underestimated there, while the theory of Milchev[24] yields an overestimate. From Wolfgardt et al.[14].

such that mesoscopic domains of A-rich and B-rich phases coexist, separated by interfaces (phase separation on a macroscopic scale can be avoided by quenching the system fast enough underneath the glass transition temperature, or by introducing chemical cross links which limit the length scale over which unmixing can occur, etc.). Since most real polymer blends contain lots of interfaces, the latter control the properties of the material, and hence a theoretical understanding of such interfaces is called for.

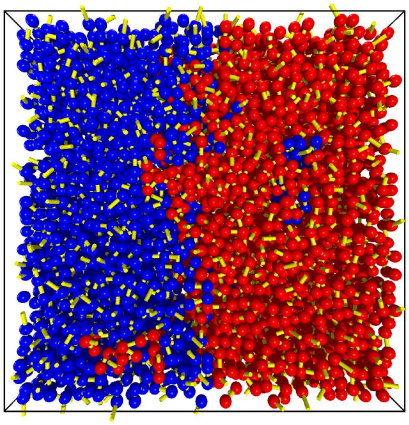

Figure 6. Snapshot picture of a binary polymer mixture (A,B), containing a single interface. A-chains are shown in red, and B-chains are shown in blue, using the bond fluctuation model for $N_A = N_B = N = 32$ and $T/T_c = 0.48$.

This problem can be addressed with the bond fluctuation model, where we allow for two types of chains (A,B) with identical chain lengths N_A, N_B and interactions $\epsilon_{AA} = \epsilon_{BB} = -\epsilon_{AB} = \epsilon$, if the two monomers are within a range of $\sqrt{6}$ lattice spacings. For this model, the bulk phase diagram could be obtained with very good precision[25]. In order to prepare a system which contains a single interface, it is convenient to use the so-called "antiperiodic boundary condition": In one lattice direction one introduces

an identity switch ($A \to B$ or $B \to A$), if a monomer crosses the system boundary in that direction. Fig. 6 shows a snapshot picture of a system prepared in this way, for the case $N_{\mathrm{A}} = N_{\mathrm{B}} = N = 32$ and a temperature far below the critical temperature T_{c} of unmixing, $T/T_{\mathrm{c}} = 0.48$. One sees that at this temperature within the coexisting domains phase separation is essentially complete, i.e. a pure A-phase coexists with a pure B-phase, intermixing occurs only in the interfacial region. Therefore it is advisable to focus on the interface behavior, and disregard the structure of the bulk phases completely. It is one of the major advantages of computer simulations, that one can extract selectively the pertinent information.

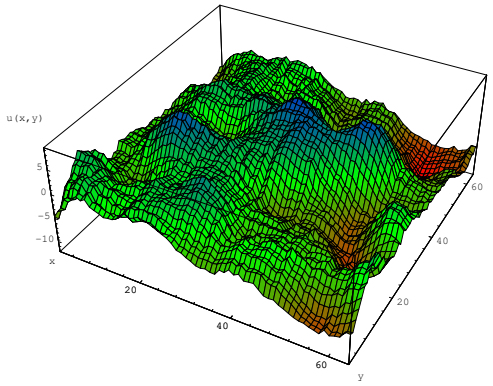

Figure 7. Snapshot picture of an instantaneous configuration of a well-equilibrated interface between an A-rich and a B-rich phase of polymers of chain lengths $N_{\mathrm{A}} = N_{\mathrm{B}} = N = 32$ at $T/T_{\mathrm{c}} = 0.48$. Here a $L \times L \times D$ geometry was chosen, with $L = 64$, $D = 64$, periodic boundary conditions in xy-directions, but antiperiodic boundary conditions in the z-direction, so that precisely one interface is stabilized in the systems. The xy-plane at $z = 0$ is divided into $B \times B$-blocks with $B = 8$, and for each block the local height $h(x, y)$ of the interface defined from the condition that the relative concentration of A and B is locally 50% is shown. From Werner et al.[16].

Fig. 7 shows a corresponding snapshot picture where just the surface representing the instantaneous position of the center of the interfacial region is shown[16]. One recognizes a "hill and valley"-type structure, i.e. there occur pronounced long wavelength fluctuations that displace the local position of the interface up and down. These interfacial fluctuations are the so-called "capillary waves", which turn out to be very pronounced for polymer mixtures, since the interfacial tension is rather small for these systems. When one averages interfacial profiles over these fluctuations, allowing for a large lateral linear dimension, the interfacial profile would seem to be much broader rather than when one takes a local average only. Thus the judgment what is attributable to the "intrinsic" interfacial profile and what is due to capillary wave broadening is rather subtle[16–18].

Nevertheless the simulations yield a wealth of illuminating information on the structure of such interfaces in polymer blends: in the interface, polymer coils get oriented parallel to the interface, and in the strong segregation limit even individual effective bonds have a preferential orientation parallel to the interface[17]. The density profile shows a dip in the center of the interface, i.e. vacancies get enriched there, and also chain ends are enriched. Knowledge of such properties is important if one wishes to discuss the mechanical strength of interfaces, chemical reactivity at interfaces, etc.

A very interesting aspect occurs when interfaces are confined in a thin film geometry (e.g. by external walls which create a binding potential acting on the interface): It then may happen that the interface at low temperatures is bound to the wall (as shown in Fig. 8),

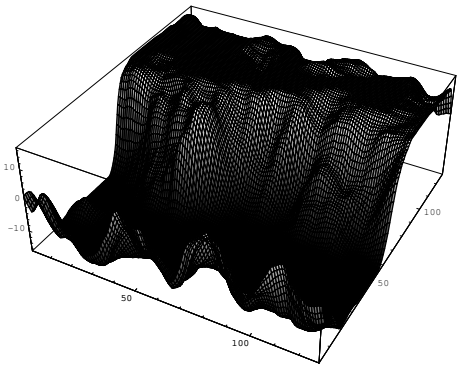

Figure 8. Snapshot picture of an instantaneous configuration of an interface between an A-rich and a B-rich phase of polymers in a thin film with "antisymmetric" walls (i.e., one wall preferentially attracts the A-monomers and the other wall attracts B-monomers with the same strength). The system geometry chosen is $128 \times 128 \times 32$, with periodic boundary conditions in x and y directions, while the two walls are located at $z = -16$ and $z = 17$, respectively. The chain length is again $N = 32$, $\epsilon_w = 0$, and the temperature $T = 0.48 T_c$.

while at higher temperatures an "interface unbinding" transition occurs. In a semi-infinite system, this is nothing but a wetting transition[18] where a macroscopically thick enrichment layer of the phase preferred by the wall forms. In a thin film geometry, the analog of wetting is the interface bound to confining walls in a thin film. When the temperature is raised, there occurs a discontinuous (= first order) transition to the situation of an unbound interface, freely fluctuating in the center of the thin film, qualitatively very similar to an interface between macroscopic coexisting phases (as shown in Fig. 7).

4 Thin Films of Block Copolymer Melts

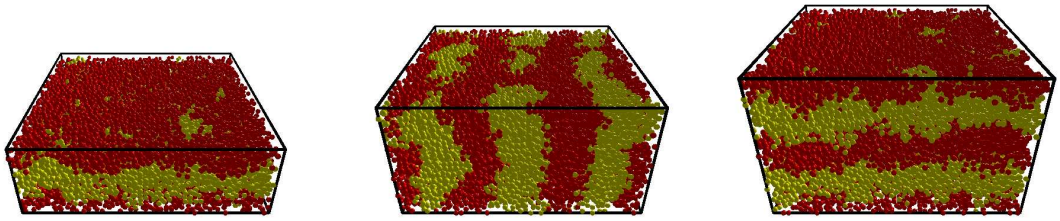

Figure 9. Snapshot pictures of the configurations of thin block copolymer films, choosing $N = 32$, $f = 1/2$, and an inverse temperature $\epsilon/k_{\mathrm{B}}T = 0.1769$ for the geometry $30 \times 96 \times 96$, $46 \times 93 \times 93$ and $56 \times 96 \times 96$, choosing the wall energy $\epsilon_{\mathrm{w}} = 0.1 k_{\mathrm{B}}T$ and periodic boundary conditions parallel to the walls. From Geisinger et al.[20].

In order to synthesize a block copolymer of composition f and chain length N, one covalently links a chain of type A (chain length N_{A}) and another chain of type B (chain length N_{B}) at one end together, to form a chain of total length $N = N_{\mathrm{A}} + N_{\mathrm{B}}$ and $f \equiv N_{\mathrm{A}}/N$[26]. As in the case of the polymer mixture, energies ϵ_{AA}, ϵ_{BB}, ϵ_{AB} between the effective monomers are present, which would lead to macroscopic phase separation between species A and B if there were not the covalent bond keeping the A-block and the B-block together: The "compromise" chosen by the system then is "microphase separation",

i.e. a periodic arrangement of A-rich and B-rich domains is formed. For compositions in the vicinity of $f = 1/2$, the arrangement of A-rich layers alternating with B-rich ones, the wavelength λ of this structure being of the same order as the gyration radius of the polymers, in the vicinity of the order-disorder transition of the block copolymer melt. Note that long range periodic order forms here in a system that is fluid, but again one can produce a solid material by performing a quench underneath the glass transition temperature.

A particularly interesting situation again occurs when one considers block copolymers in thin film geometry, confined between two parallel walls at a distance D[27]. Normally, there will be a preferential attraction of one of the blocks to the walls, causing hence an arrangement of the lamellae parallel to the confining walls. However, the lamellar arrangement will nicely fit into the thin film only if the wavelength λ and the film thickness D are commensurate, and there is no reason that this holds true in general (note that λ depends both on N and on temperature[26]). In the case of strong incommensurability, it becomes energetically preferable to orient the lamellae perpendicular to the walls rather than parallel, and such a perpendicular orientation has been observed both experimentally and by computer simulations[20], see Fig. 9. The perpendicular oriented morphology has attracted abiding interest as a template for laterally structured devices on the nanometer scale. Simulations as shown in Fig. 9 are very important, since they allow a better understanding of the conditions for which this perpendicular ordering is stable.

Of course, due to the low temperatures necessary for this ordering the relaxation times are very long, and runs of a length of several million Monte Carlo steps are required. For the rather large lattices used in Figs. 6-9 a use of CRAY-T3E supercomputers again is mandatory, making use of a strip-like domain decomposition parallel to the walls for an efficient use of up to 64 processors in parallel.

5 Concluding Remarks

Three examples have been discussed in order to show that the large scale simulation of simple models for polymer chains yields valuable insight in the phase transitions that occur in polymeric materials, namely the glass transition, unmixing of symmetric polymer blends, particular in confined geometry, and mesophase order-disorder transitions of thin block copolymer films. All these phase transitions at the same time are challenging problems of soft matter physics and important from the point of view of materials research. Thus, the results (described in more detail in the original papers[2–20]) have both elucidated controversial theoretical questions and stimulated experiments. Nevertheless it is clear that such work is a first step only – we still lack the possibility to predict the properties of specific polymeric materials (e.g. where the glass transition of a particular polymer occurs, and how we can change it when we modify the chemical structure), and also on a qualitative level fascinating problems are still out of reach, such as the interplay of phase separation and glassification, or the more complex ordering of multiblock copolymers and the interplay between phase separation and ordering in mixtures of different block copolymers, etc. Such problems will become accessible only with the next generation of even more powerful supercomputers.

Acknowledgments

We thank M. Aichele, C. Bennemann, B. Dünweg, T. Geisinger, L. G. MacDowell, F. Schmid, A. Werner, and M. Wolfgardt for their fruitful collaboration on the problems described here. This research was supported by the Deutsche Forschungsgemeinschaft (DFG) under grants No SFB262/D2, Bi314/3, Bi314/17 and the Bundesministerium für Bildung und Forschung (BMBF) under grants No 03N8008C and 03N6015. We are particularly grateful to the NIC Jülich and the HLRS Stuttgart for generous allocations of computer time on CRAY-T3E supercomputers.

References

1. P. G. deGennes, Scaling Concepts in Polymer Physics, Cornell University Press, Ithaca, N.Y. 1979.
2. C. Bennemann, W. Paul, K. Binder and B. Dünweg, Phys. Rev. E**57**, 843 (1998).
3. C. Bennemann, J. Baschnagel, W. Paul, and K. Binder, Comput. Theor. Pol. Sci. **9**, 217 (1999).
4. C. Bennemann, J. Baschnagel, and W. Paul, Eur. Phys. J B**10**, 323 (1999).
5. C. Bennemann, W. Paul, J. Baschnagel, and K. Binder, J. Phys.: Condens. Matter **11**, 2179 (1999).
6. J. Baschnagel, C. Bennemann, W. Paul and K. Binder, J. Phys.: Condens. Matter **12**, 6365 (2000).
7. M. Aichele and J. Baschnagel, Eur. J. Phys. E**5**, 229, 245 (2001).
8. K. Binder, J. Baschnagel and W. Paul, Progr. Polymer Sci. (2002, in press).
9. M. Müller and L. G. MacDowell, Macromolecules **33**, 3902 (2000).
10. M. Müller and L. G. MacDowell, Europhys. Lett. **55**, 221 (2001).
11. K. Binder, in *Monte Carlo and Molecular Dynamics Simulations in Polymer Science* (Oxford University Press, N. Y. 1995) ed. by K. Binder, p. 1.
12. J. Baschnagel, K. Binder and H.-P. Wittmann, J. Phys.: Condens. Matter **5**, 1597 (1993).
13. W. Paul and J. Baschnagel, in Ref.[11], p. 307.
14. M. Wolfgardt, J. Baschnagel, W. Paul and K. Binder, Phys. Rev. E**54**, 1535 (1996).
15. H.-P. Deutsch and K. Binder, J. Chem. Phys. **94**, 2294 (1991).
16. A. Werner, F. Schmid, M. Müller, and K. Binder, J. Chem. Phys. **107**, 8175 (1997).
17. A. Werner, F. Schmid, M. Müller, and K. Binder, Phys. Rev. E**59**, 728 (1999).
18. M. Müller and K. Binder, Macromolecules **31**, 8323 (1998).
19. M. Müller and K. Binder, Phys. Rev. E**63**, 021602 (2001).
20. T. Geisinger, M. Müller, and K. Binder, J. Chem. Phys. **111**, 5241, 5251 (1999).
21. W. Götze and S. Sjögren, Rep. Progr. Phys. **55**, 214 (1992).
22. J. H. Gibbs and E. A. di Marzio, J. Chem. Phys. **28**, 373 (1958).
23. P. J. Flory, Proc. Roy. Soc. London A**234**, 60 (1956).
24. A. Milchev, C. R. Acad. Bulg. Sci. **36**, 1415 (1983).
25. H.-P. Deutsch and K. Binder, Macromolecules **25**, 6214 (1992).
26. K. Binder, Adv. Polymer Sci. **112**, 181 (1994).
27. K. Binder, Adv. Polymer Sci. **138**, 1 (1999).